ACS Medicinal Chemistry Letters

Letter

pubs.acs.org/acsmedchemlett

Discovery of Dabrafenib: A Selective Inhibitor of Raf Kinases with Antitumor Activity against B-Raf-Driven Tumors

Tara R. Rheault,*[,†] John C. Stellwagen,[†] George M. Adjabeng,[†] Keith R. Hornberger,[†] Kimberly G. Petrov,[†] Alex G. Waterson,[†] Scott H. Dickerson,[∥] Robert A. Mook, Jr.,[†] Sylvie G. Laquerre,[‡] Alastair J. King,[‡] Olivia W. Rossanese,[‡] Marc R. Arnone,[‡] Kimberly N. Smitheman,[‡] Laurie S. Kane-Carson,[§] Chao Han,[‡] Ganesh S. Moorthy,[‡] Katherine G. Moss,[‡] and David E. Uehling[†]

[†]Oncology R&D Medicinal Chemistry, GlaxoSmithKline, Research Triangle Park , North Carolina 27709, United States

[‡]Oncology R&D Cancer Research, GlaxoSmithKline, Collegeville Road, Collegeville, Pennsylvania 19426, United States

[§]Platform Technology & Science, GlaxoSmithKline, Research Triangle Park, North Carolina 27709, United States

[∥]Computational and Structural Chemistry, GlaxoSmithKline, Research Triangle Park, North Carolina 27709, United States

Supporting Information

ABSTRACT: Hyperactive signaling of the MAP kinase pathway resulting from the constitutively active B-Raf^{V600E} mutated enzyme has been observed in a number of human tumors, including melanomas. Herein we report the discovery and biological evaluation of GSK2118436, a selective inhibitor of Raf kinases with potent in vitro activity in oncogenic B-Raf-driven melanoma and colorectal carcinoma cells and robust in vivo antitumor and pharmacodynamic activity in mouse models of B-Raf^{V600E} human melanoma. GSK2118436 was identified as a development candidate, and early clinical results have shown significant activity in patients with B-Raf mutant melanoma.

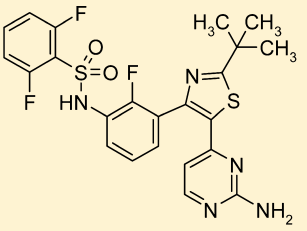

dabrafenib

B-Raf IC_{50} = 0.7 nM
pERK IC_{50} (SKMEL28) = 4 nM
SKMEL28 IC_{50} = 3 nM
A375P F11 IC_{50} = 8 nM
Colo205 IC_{50} = 7 nM

KEYWORDS: *B-Raf, GSK2118436, dabrafenib, melanoma, MAP kinase*

The MAP kinase pathway plays a central role in cellular growth processes, and aberrant signaling through this pathway has been observed in many cancers.[1−4] Notably, activating mutations in B-Raf have been identified in more than 60% of all melanomas.[1] The most common mutation, observed in 80−90% of B-Raf mutant cancers, is the B-Raf^{V600E} mutation, which renders the kinase constitutively active. This mutation, which substitutes valine with glutamic acid at amino acid 600 in the activation loop, mimics regulatory phosphorylation and results in in vitro kinase activity of the protein being 500-fold greater than that of wild-type B-Raf.[1,5] Because tumors bearing an activating B-Raf^{V600E} mutation show oncogenic addiction to this hyperactivated signaling pathway, it was postulated that small molecule inhibitors of B-Raf^{V600E} kinase activity offer a novel, targeted approach for the treatment of B-Raf^{V600E}-driven cancers.[6] This hypothesis has since been tested clinically, and significant responses to selective B-Raf inhibitor therapy have been observed.[7]

Herein we describe the medicinal chemistry efforts leading to the discovery of GSK2118436 (dabrafenib), a potent, selective, and efficacious inhibitor of B-Raf^{V600E}. GSK2118436 is currently in phase III clinical development for the treatment of activating B-Raf mutant tumors.

Our early efforts aimed at discovering inhibitors of B-Raf^{V600E} suitable for clinical evaluation led to the identification of thiazole **1**.[8] This compound shows potent in vitro kinase inhibitory activity against the B-Raf^{V600E} enzyme, and in both cellular mechanistic (pERK) and proliferation assays in the B-Raf^{V600E} SKMEL28 melanoma cell line (Table 1). Thiazole **1** also had low clearance and good overall oral systemic exposure in rats. However, this compound displayed very high clearance and poor bioavailability in nonrodent species. Additionally, metabolite identification studies conducted in dog and monkey liver microsomes identified several major metabolites clustered in the tail and core regions of the molecule. We hypothesized that drug exposure after an oral dose in the higher species was limited by rapid compound metabolism. Medicinal chemistry efforts were thus focused on improving pharmacokinetic properties in dog while preserving the favorable target potency, selectivity, and rodent pharmacokinetic properties inherent in this template.[9]

Having established the sulfonamide as a key pharmacophore required for potent cellular inhibition of B-Raf^{V600E}, we performed significant structural modifications elsewhere to lower the molecular weight and reduce the number of metabolic sites contained within the template. Truncation of the tail by replacing the aminopyridine in **1** with a small alkyl

Received: January 12, 2013
Accepted: February 7, 2013

   dx.doi.org/10.1021/ml4000063 | *ACS Med. Chem. Lett.* XXXX, XXX, XXX−XXX

Table 1. Structure, in Vitro Data, and Pharmacokinetic Data for Compound 1 in Rat, Dog, and Monkey

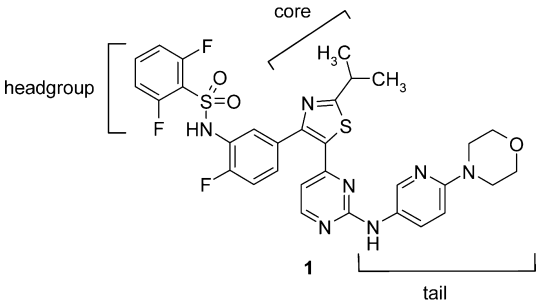

B-Raf^{V600E} IC_{50} (nM)	pERK IC_{50} (nM)	SKMEL28 proliferation IC_{50} (nM)	species	intrinsic Cl_i[a]	Cl[b]	po DNAUC[c]	% F
3.8	23	48	rat	9	9[d]	1748[d]	85
			dog	53	38[e]	42[e]	10
			monkey	8	39[e]	23[e]	5

[a]Intrinsic clearance data from liver microsomes, reported in units of milliliters per minute per gram of liver. [b]Intravenous blood clearance reported in units of milliliters per minute per kilogram. [c]Oral dose-normalized AUC (DNAUC) reported as nanograms hour per milliliter per milligram per kilogram (n = 3). [d]Dosing vehicle: 1% DMSO, 10% solutol in saline or water, at pH 5.0. [e]Dosing vehicle: 1% DMSO, 30% PEG400 in saline or water, at pH 3.5−4.5.

Table 2. Truncated Tail SAR

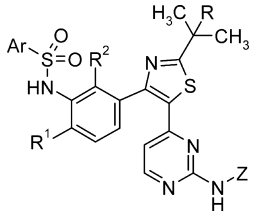

Compound	Ar-substitution	R^1	R^2	R	Z	B-Raf^{V600E} IC_{50} (nM)[a]	pERK IC_{50} (nM)[b]	SKMEL28 proliferation IC_{50} (nM)[c]	Rat Cl[d,e,g]	Rat po DNAUC[d,e,g]	Dog Cl[d,e,h]	Dog po DNAUC[d,e,h]
2	2,6-difluorophenyl	H	H	H	H	40	78	641	121	23	NT[f]	NT[f]
3	2,5-difluorophenyl	H	H	Me	H	8	7	69	110	27	NT[f]	NT[f]
4	3-fluorophenyl	F	H	H	H	536	2555	15716	NT[f]	NT[f]	NT[f]	NT[f]
5	3-fluorophenyl	H	H	H		32	28	671	154	16	NT[f]	NT[f]
6	3-fluorophenyl	H	H	H	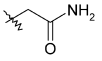	11	26	217	109	6	NT[f]	NT[f]
7	3-fluorophenyl	H	H	H	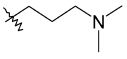	28	73	1292	NT[f]	NT[f]	NT[f]	NT[f]
8	2,6-difluorophenyl	H	H	H	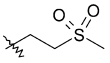	1	4	10	84	34	NT[f]	NT[f]
9	2,6-difluorophenyl	F	H	H	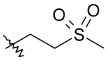	13	51	266	13	1024	56	43
10	2,6-difluorophenyl	H	F	H	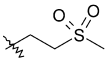	0.3	7	10	36	125	47	68
11	2,6-difluorophenyl	F	H	CH_3	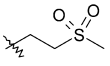	13	11	87	16	1373	NT[f]	NT[f]
12	2,6-difluorophenyl	H	F	CH_3	H	0.7	4	3	18	729	4	3754

[a]B-Raf^{V600E} enzymatic activity. Values are means of at least two experiments; individual values are within 2-fold of the reported mean value. [b]Inhibition of pERK in SKMEL28 cells. Values are means of at least two experiments; individual values are within 2-fold of the reported mean value. [c]Inhibition of SKMEL28 cell proliferation. IC_{50} values are means of at least experiments; individual values are within 3-fold of the reported mean value. [d]Intravenous clearance reported in units of milliliters per minute per kilogram. Oral dose-normalized AUC (DNAUC) reported as nanograms hours per milliliter per milligram per kilogram (n = 3). [e]Data from four-compound cassette dosing. Pharmacokinetic values based on cassette dosing were found to be within 2-fold of those of discretely dosed experiments. [f]Not tested. [g]Dosing vehicle: 1% DMSO, 10% solutol in saline or water, at pH 5.0. [h]Dosing vehicle: 1% DMSO, 30% PEG400 in saline or water, at pH 3.5−4.5.

group (**5**) or polar functionality (**6**−**8**) largely preserved enzyme potency, cellular mechanistic potency (pERK), and inhibition of proliferation in B-Raf^{V600E} SKMEL28 cells but resulted in significantly higher clearance in rat (Table 2).[10]

dx.doi.org/10.1021/ml4000063 | ACS Med. Chem. Lett. XXXX, XXX, XXX−XXX

Surprisingly, unsubstituted aminopyrimidine hinge binder (**2**) maintained in vitro potency against B-Raf;[11] however, this compound also demonstrated high in vivo clearance in rat. Core group modifications were attempted in an effort to alter the metabolic stability of this series, leading to a *tert*-butyl core analogue (**3**). While this change from isopropyl to *tert*-butyl resulted in a noteworthy increase in potency, rat intravenous (iv) clearance was still very high and oral exposure was commensurately low. Since fluoro substitution at position 6 of the phenyl ring [R^1 = F (Table 2)] led to an important improvement in rat pharmacokinetic properties in previous SAR efforts,[8] this substitution was attempted in the truncated tail series (**4**). Unfortunately, in this context, fluoro substitution at R^1, when combined with the tail truncation, led to a decrease in potency such that further progression of compound **4** was abandoned.

Given the favorable potency demonstrated with compound **8**, SAR in this series was further explored. In an effort to lower IV clearance in rats, compounds with substitution at positions R, R^1, and R^2 were prepared and evaluated. Fluorination at R^1 (**9**) decreased the enzyme and cellular potency but resulted in a marked improvement in rat iv clearance and oral exposure. Further SAR on this template showed that fluorination at R^2 (**10**) improved or maintained the enzyme and cellular potency and resulted in improved pharmacokinetic properties compared to those of the des-fluoro analogue (**8**). Replacement of the isopropyl thiazole core with a *tert*-butyl thiazole core (**11**) also resulted in improved cellular potency. While rat pharmacokinetic properties could be improved by extrapolating previous SAR findings from this series, analogous improvements in dog pharmacokinetic properties were not realized, as compounds **9** and **10** both displayed high clearance and poor oral exposure in dog.

Further attempts to optimize pharmacokinetic properties while maintaining potency in this series were made by combining the structural modifications of fluorination at R^2, replacing the isopropyl core with a *tert*-butyl group, and utilizing the unsubstituted aminopyrimidine tail group from compounds **2**–**4**. Through this effort, compound **12** (GSK2118436) was synthesized and evaluated (Table 2 and Figure 1).

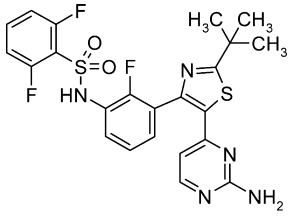

12

Figure 1. Dabrafenib (GSK2118436).

GSK2118436 (**12**) displayed compelling inhibitory activity in enzyme and cellular mechanistic assays, and in cell proliferation assays in B-Raf^{V600E}-driven melanoma lines, SKMEL28 and A375P F11 (IC_{50} = 3 and 8 nM, respectively), and colorectal carcinoma line Colo205 (IC_{50} = 7 nM). Gratifyingly, GSK2118436 was found to have a minimal effect in vitro on cells with wild-type B-Raf (HFF IC_{50} = 3.0 μM) and in tumor cells not harboring the activating B-Raf^{V600E} mutation.[12] Additionally, acceptable rat and dramatically improved dog pharmacokinetic profiles were observed, in contrast to those of previously prepared analogues.

The remarkable improvement in dog pharmacokinetic properties prompted further investigation in order to understand the rationale for the finding. In an effort to understand the high clearance observed in dog from sulfone-containing tail compounds (Table 2), **9** was incubated in dog hepatocytes and the major metabolites were identified by mass spectrometry (Figure 2). Following incubation of compound **9** in dog

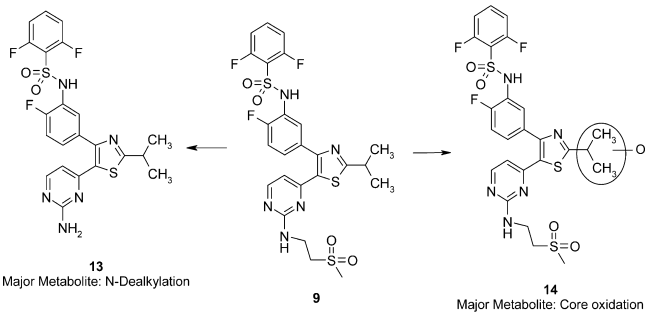

Figure 2. Metabolite identification of **9** in dog hepatocytes.

hepatocytes, two major metabolites were identified: compound **13**, showing complete dealkylation of the ethylmethylsulfone tail, and compound **14**, a product of oxidation of the isopropyl core. In retrospect, it was surmised that removal of the tail group and replacement of the isopropyl core group with a *tert*-butyl attenuated the metabolic liabilities associated with these positions and led to the significant improvements in the dog pharmacokinetic properties of **12**.

GSK2118436 was screened against a set of 61 kinases representing broad coverage of the kinome and was found to be a potent biochemical inhibitor of B-Raf^{V600E}, wild-type B-Raf, and c-Raf, displaying subnanomolar or nanomolar potencies (see the Supporting Information). Importantly, GSK2118436 was also found to be highly selective, exhibiting >500-fold selectivity for B-Raf^{V600E} compared to most kinases screened.[13] Significant activity (<100-fold selectivity) was observed for a single kinase in the panel, Alk5. The impact of Alk5 enzyme activity on cellular signaling was further investigated by measuring the downstream phosphorylation level of SMAD2/3 in HepG2 cells.[14] GSK2118436 was significantly less effective at inhibiting SMAD2/3 phosphorylation (IC_{50} = 3.7 μM) compared with inhibiting ERK phosphorylation (IC_{50} = 4 nM) in a cellular context. These data underscore the remarkable selectivity achieved by this uniquely potent and selective inhibitor of B-Raf^{V600E}.

GSK2118436 was also studied in vivo and found to dramatically reduce tumor growth in mice bearing B-Raf^{V600E} human melanoma tumors. In this model, CD1 *nu*/*nu* mice bearing A375P F11 (B-Raf^{V600E}) tumors were dosed orally with GSK2118436 at doses of 0.1, 1, 10, and 100 mg/kg once daily for 14 days (Figure 3). Dose-proportional reductions in tumor growth were observed. Body weight was also measured, and no significant changes were observed at any of the doses tested. Notably, in the 100 mg/kg group, complete tumor regression was observed in 50% of treated animals.

Additionally, GSK2118436 reduced the levels of pERK in A375P F11 (B-Raf^{V600E}) tumor tissue in vivo in a dose-dependent manner after a single oral dose. Tumors were collected 2, 6, and 24 h postdose, and pERK levels in each were

dx.doi.org/10.1021/ml4000063 | ACS Med. Chem. Lett. XXXX, XXX, XXX–XXX

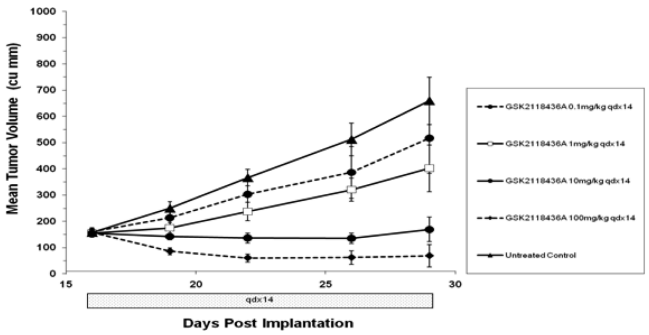

Figure 3. In vivo efficacy of GSK2118436 in CD1 *nu/nu* mice bearing A375P F11 (B-Raf^{V600E}) tumors (n = 8 per group).

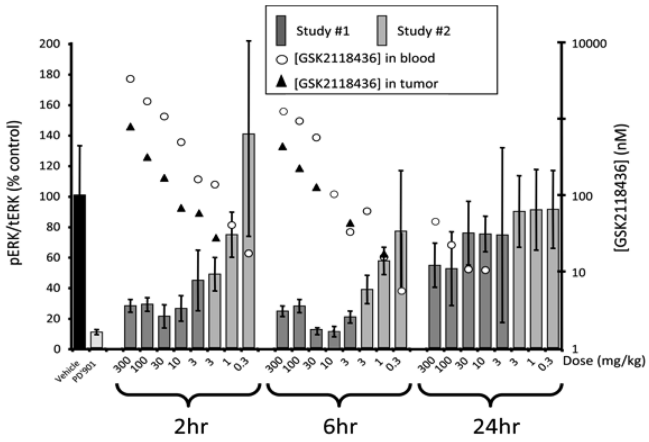

Figure 4. In vivo pharmacodynamic response of a single dose of GSK2118436 in CD1 *nu/nu* mice bearing A375P F11 (B-Raf^{V600E}) tumors (n = 4 per group).

measured and normalized to the total ERK (tERK) present. The MEK inhibitor PD0325901 was used as a control. Figure 4 shows pERK/tERK levels compared to those of vehicle-treated animals and pharmacokinetic data in a composite of two separate studies. Levels of pERK/tERK were substantially reduced 2 and 6 h postdose, with a notable pharmacodynamic effect (>50% inhibition) at doses of ≥3 mg/kg in this single-dose study, which returned to untreated levels by 24 h at doses of ≤30 mg/kg. The concentration of drug measured in the blood and tumor during the course of the study correlated with the observed pharmacodynamic effects. These data suggest that under the conditions tested, a single oral dose of ≥3 mg/kg GSK2118436 can maintain ≥50% B-Raf inhibition for at least 6 h.

In summary, lead molecule **1**, with high potency and poor pharmacokinetic properties in higher species, was rapidly evolved into clinical development candidate GSK2118436 (**12**). Identification of the key B-Raf^{V600E} potency contributors (sulfonamide head, R^2 fluorination, and *tert*-butyl thiazole core) through detailed and iterative SAR studies allowed for the elimination of nonessential portions of the lead structure and high selectivity to be achieved across the kinome. With high enzyme and cellular potency engineered into the original lead, pharmacokinetic issues were addressed by combining multiple changes in the template, resulting in the improved multispecies PK properties observed for **12**. With high rodent exposure realized in GSK2118436, we were able to demonstrate target-related pharmacology in two in vivo models, gaining a high level of confidence in the progression of this molecule into clinical studies. Additionally, vast improvements in higher-species PK allowed for the achievement of exposures necessary to fully explore the safety of the molecule preclinically. Finally, a >20% decrease in molecular weight compared to that of **1** resulted in improved physicochemical properties, expediting the identification of a salt version (mesylate) and form suitable for early clinical studies.

The efforts described herein ultimately led to the discovery of GSK2118436 (dabrafenib), which is currently in advanced clinical studies in B-Raf mutant tumors. GSK2118436 has shown remarkable efficacy in melanoma patients with activating B-Raf mutations, including patients with brain metastases, and has further shown enhanced clinical activity in combination with the MEK inhibitor, trametinib.[15−17] Details of these studies will be reported in due course.

■ ASSOCIATED CONTENT

Supporting Information

Biochemical and cellular assays, metabolite identification experimental procedures, kinase selectivity data, A375P F11 melanoma xenograft, PK analysis, pharmacodynamic measurement of pERK in tissues, and experimental procedures for the compounds and characterization of dabrafenib. This material is available free of charge via the Internet at http://pubs.acs.org.

■ AUTHOR INFORMATION

Corresponding Author

*E-mail: tara.r.rheault@gsk.com.

Notes

The authors declare the following competing financial interests: T.R.R., S.H.D., K.G.P., S.G.L., M.R.A., K.N.S., L.S.K.-C., and K.G.M. are current employees and stockholders of GlaxoSmithKline.

All studies involving the use of animals were conducted after review by the GlaxoSmithKline (GSK) Institutional Animal Care and Use Committee and in accordance with the GSK Policy on the Care, Welfare and Treatment of Laboratory Animals.

■ ACKNOWLEDGMENTS

The authors thank Erich Baum, Neil Bifulco, Ronda Davis-Ward, Kelly Donaldson, Kyle Emmitte, Phil Harris, Kevin Kuntz, Kristen Nailor, Jim Salovich, Doug Sammond, Greg Schaaf, Stephon Smith, and Brian Wilson for scientific support and Dash Dhanak and Dirk Heerding for critically reviewing the manuscript and support throughout the duration of the program.

■ REFERENCES

(1) Davies, H.; Bignell, G.; Cox, C.; Stevens, P.; Edkins, S.; Clegg, S.; Teague, J.; Woffendin, H.; Garnett, M.; Bottomley, W.; Davis, N.; Dicks, E.; Ewing, R.; Floyd, Y.; Gray, K.; Hall, S.; Hawes, R.; Hughes, J.; Kosmidou, V.; Menzies, A.; Mould, C.; Parker, A.; Stevens, C.; Watt, S.; Hooper, S.; Wilson, R.; Jayatilake, H.; Gusterson, B.; Cooper, C.; Shipley, J.; Hargrave, D.; Pritchard-Jones, K.; Maitland, N.; Chenevix-Trench, G.; Riggins, G.; Bigner, D.; Palmieri, G.; Cossu, A.; Flanagan, A.; Nicholson, A.; Ho, J.; Leung, S.; Yuen, S.; Weber, B.; Seigler, H.; Darrow, T.; Paterson, H.; Marais, R.; Marshall, C.; Wooster, R.; Stratton, M.; Futreal, P. Mutations of the BRAF gene in human cancer. *Nature* **2002**, *417*, 949−954.

(2) Singer, G.; Oldt, R.; Cohen, Y.; Wang, B.; Sidransky, D.; Kurman, R.; Shih, Ie. M. Mutations in BRAF and KRAS characterize the development of low-grade ovarian serous carcinoma. *J. Natl. Cancer Inst.* **2003**, *95*, 484−486.

(3) Cohen, Y.; Xing, M.; Mambo, E.; Guo, Z.; Wu, G.; Trink, B.; Beller, U.; Westra, W. H.; Ladenson, P. W.; Sidransky, D. BRAF mutation in papillary thyroid carcinoma. *J. Natl. Cancer Inst.* **2003**, *95*, 625−627.
(4) Yuen, S.; Davies, H.; Chan, T.; Ho, J.; Bignell, G.; Cox, C.; Stephens, P.; Edkins, S.; Tsui, W.; Chan, A.; Futreal, P.; Stratton, M.; Wooster, R.; Leung, S. Similarity of the phenotypic patterns associated with BRAF and KRAS mutations in colorectal neoplasia. *Cancer Res.* **2002**, *62*, 6451−6455.
(5) Wan, P.; Garnett, M.; Roe, S.; Lee, S.; Niculescu-Duvaz, D.; Good, V.; Jones, C. M.; Marshall, C. J.; Springer, C. J.; Barford, D.; Marais, R. Mechanism of Action of the RAF-ERK Signaling Pathway by Oncogenic Mutations of B-RAF. *Cell* **2004**, *116*, 855−867.
(6) Tsai, J.; Lee, J.; Wang, W.; Zhang, J.; Cho, H.; Mamo, S.; Bremer, R.; Gillette, S.; Kong, J.; Haass, N.; Sproesser, K.; Li, L.; Smalley, K.; Fong, D.; Zhu, Y.-L.; Marimuthu, A.; Nguyen, H.; Lam, W.; Liu, J.; Cheung, I.; Rice, J.; Suzuki, Y.; Luu, C.; Settachatgul, C.; Shellooe, R.; Cantwell, J.; Kim, S.-H.; Schlessinger, J.; Zhang, K.; West, B.; Powell, B.; Habets, G.; Zhang, C.; Ibrahim, P.; Hirth, P.; Artis, D.; Herlyn, M.; Bollag, G. Discovery of a selective inhibitor of oncogenic B-Raf kinase with potent antimelanoma activity. *Proc. Natl. Acad. Sci. U.S.A.* **2008**, *105*, 3041−3046.
(7) Chapman, P.; Hauschild, A.; Robert, C.; Haanen, J.; Ascierto, P.; Larkin, J.; Dummer, R.; Garbe, C.; Testori, A.; Maio, M.; Hogg, D.; Lorigan, P.; Lebbe, C.; Jouary, T.; Schadendorf, D.; Ribas, A.; O'Day, S.; Sosman, J.; Kirkwood, J.; Eggermont, A.; Dreno, B.; Nolop, K.; Li, J.; Nelson, B.; Hou, J.; Lee, R.; Flaherty, K. Improved survival with vemurafenib in melanoma with BRAF V600E mutation. *N. Engl. J. Med.* **2011**, *364*, 2507−2516.
(8) Stellwagen, J.; Adjabeng, G.; Arnone, M.; Dickerson, S.; Han, C.; Hornberger, K.; King, A.; Mook, R.; Petrov, K.; Rheault, T.; Rominger, C.; Rossanese, O.; Smitheman, K.; Waterson, A.; Uehling, D. Development of Potent B-Raf^{V600E} Inhibitors Containing an Arylsulfonamide Headgroup. *Bioorg. Med. Chem. Lett.* **2011**, *21*, 4436−4440.
(9) Efforts were focused on optimizing pharmacokinetic properties in rat and dog to identify two species for preclinical safety studies.
(10) Previously, we reported that fluorination of the arylsulfonamide headgroup at the 2-, 3-, 2,5-, and 2,6-positions gave optimal, and nearly interchangeable, potency in this series. Additionally, in vivo pharmacokinetic studies in rat and dog with similarly paired analogues showed that changes in the headgroup substitution pattern had little impact on either clearance or oral absorption. Thus, potency and pharmacokinetic properties observed in this series do not appear to be sensitive to changes in the fluorination pattern of the headgroup. See ref 8.
(11) For a discussion of the binding efficiency of truncated tail-containing molecule **2** compared to **1** in the context of the B-Raf binding mode, see the Supporting Information.
(12) For a thorough biological characterization of dabrafenib, see: King, A.; Arnone, M.; Bleam, M.; Moss, K.; Yang, J.; Fisher, K.; Smitheman, K.; Erhardt, J.; Hughes-Earle, A.; Kane-Carson, L.; Sinnamon, R.; Qi, H.; Rheault, T.; Uehling, D.; Laquerre, S. Novel Selective BRAF Inhibitor (GSK2118436; dabrafenib) with Demonstration of Increased Efficacy and Reduced Skin Lesions by Combining BRAF and MEK Inhibitors. Manuscript in preparation.
(13) Broader kinase profiling was recently conducted on a set of 270 kinases (Millipore), and <100-fold activity was observed for only LIMK1, NEK11, PKD2, and SIK in addition to ALK5. See ref 12.
(14) Gellibert, F.; de Gouville, A.-C.; Woolven, J.; Mathews, N.; Nguyen, V.-L.; Bertho-Ruault, C.; Patikis, A.; Grygielko, E.; Laping, N.; Huet, S. Discovery of 4-{4-[3-(Pyridin-2-yl)-1H-pyrazol-4-yl]-pyridin-2-yl}-N-(tetrahydro-2H-pyran-4-yl)benzamide (GW788388): A Potent, Selective, and Orally Active Transforming Growth Factor-β Type I Receptor Inhibitor. *J. Med. Chem.* **2006**, *49*, 2210−2221.
(15) Hauschild, A.; Grob, J.; Demidov, L.; Jouary, T.; Gutzmer, R.; Millward, M.; Rutkowski, P.; Blank, C.; Miller, W.; Kaempgen, E.; Martín-Algarra, S.; Karaszewska, B.; Mauch, C.; Chiarion-Sileni, V.; Martin, A.; Swann, S.; Haney, P.; Mirakhur, B.; Guckert, M.; Goodman, V.; Chapman, P. Dabrafenib in BRAF-mutated metastatic melanoma: A multicentre, open-label, phase 3 randomised controlled trial. *Lancet* **2012**, *380*, 358−365.
(16) Falchook, G.; Long, G.; Kurzrock, R.; Kim, K.; Arkenau, T.; Brown, M.; Hamid, O.; Infante, J.; Millward, M.; Pavlick, A.; O'Day, S.; Blackman, S.; Curtis, C.; Lebowitz, P.; Ma, B.; Ouellet, D.; Kefford, R. Dabrafenib in patients with melanoma, untreated brain metastases, and other solid tumours: a phase 1 dose-escalation trial. *Lancet* **2012**, *379*, 1893−1901.
(17) Weber, J.; Flaherty, K.; Infante, J.; Falchook, G.; Kefford, R.; Daud, A.; Hamid, O.; Gonzalez, R.; Kudchadkar, R.; Lawrence, D.; Burris, H.; Long, G.; Algazi, A.; Lewis, K.; Kim, K.; Puzanov, I.; Sun, P.; Little, S.; Patel, K.; Sosman, J. Updated safety and efficacy results from a phase I/II study of the oral BRAF inhibitor dabrafenib (GSK2118436) combined with the oral MEK 1/2 inhibitor trametinib (GSK1120212) in patients with BRAFi-naive metastatic melanoma. *ASCO Meeting Abstracts* **2012**, *30*, 8510.